SONIC HEDGEHOG GENE ENHANCED TISSUE ENGINEERING FOR BONE REGENERATION

Paul C. Edwards MSc, DDS[1], Salvatore Ruggiero DMD, MD[2], John Fantasia DDS[3], Ronald Burakoff DMD[4], Sameer M. Moorji BS[5], Pasquale Razzano MA[5], Daniel A. Grande PhD[6], and James M. Mason PhD[7]

[1] Resident, Division of Oral and Maxillofacial Pathology, Department of Dental Medicine, Long Island Jewish Medical Center, 270-05 76th Avenue, New Hyde Park, NY, 11040,

[2] Chief, Division of Oral and Maxillofacial Surgery, Department of Dental Medicine, Long Island Jewish Medical Center, 270-05 76th Avenue, New Hyde Park, NY, 11040,

[3] Chief, Division of Oral and Maxillofacial Pathology, Department of Dental Medicine, Long Island Jewish Medical Center, 270-05 76th Avenue, New Hyde Park, NY, 11040,

[4] Chairman, Department of Dental Medicine, Long Island Jewish Medical Center, 270-05 76th Avenue, New Hyde Park, NY, 11040,

Accepted Author's Manuscript. Final version published as:

Edwards, P. C., Ruggiero, S., Fantasia, J., Burakoff, R., Moorji, S. M., Paric, E., … Mason, J. M. (2004). Sonic hedgehog gene-enhanced tissue engineering for bone regeneration. Gene Therapy, 12(1), 75–86. http://dx.doi.org/10.1038/sj.gt.3302386

[5] Research Assistant, Gene Therapy Vector and Orthopedic

Research Laboratories,

North Shore- Long Island Jewish Research Institute, 350 Community Drive,

Manhasset NY 11030,

[6] Director, Orthopedic Research, Department of Orthopedic Surgery,

North Shore- Long Island Jewish Research Institute, 350 Community Drive,

Manhasset NY 11030, and

[7] Director, Gene Therapy Vector Laboratory,

North Shore- Long Island Jewish Research Institute, 350 Community Drive,

Manhasset NY 11030.

Correspondence to:

Dr. James M. Mason,

Director, Gene Therapy Vector Laboratory

North Shore- Long Island Jewish Research Institute,

350 Community Drive,

Manhasset NY 11030

KEYWORDS

sonic hedgehog; shh; gene-enhanced bone regeneration; bone regeneration; retroviral expression vector; gingival fibroblasts; fat-derived stem cells; periosteal-derived cells; alginate; bovine collagen

WORD COUNT

5017

Paul C. Edwards MSc, DDS

Resident, Division of Oral and Maxillofacial Pathology,

Department of Dental Medicine,

Long Island Jewish Medical Center,

270-05 76th Avenue, New Hyde Park, NY, 11040

Tel: (718)-470-7120

Fax: (718)-347-3403

E-mail: pedwards@lij.edu

Salvatore Ruggiero DMD, MD

Chief, Division of Oral and Maxillofacial Surgery,

Department of Dental Medicine,

Long Island Jewish Medical Center,

270-05 76th Avenue, New Hyde Park, NY, 11040

Tel: (718)-470-7120

Fax: (718)-347-3403

E-mail: ruggiero@lij.edu

John Fantasia DDS

Chief, Division of Oral and Maxillofacial Pathology,

Department of Dental Medicine,

Long Island Jewish Medical Center,

270-05 76th Avenue, New Hyde Park, NY, 11040

Tel: (718)-470-7120

Fax: (718)-347-3403

E-mail: fantasia@lij.edu

Ronald Burakoff DMD

Chairman, Department of Dental Medicine,

Long Island Jewish Medical Center,

270-05 76th Avenue, New Hyde Park, NY, 11040

Tel: (718)-470-7111

Fax: (718)-347-4118

E-mail: rburakof@lij.edu

Sameer M. Moorji BS

Research Assistant, Gene Therapy Vector Laboratory

North Shore- Long Island Jewish Research Institute

350 Community Drive, Manhasset NY 11030

(516) 562-1141 (Office)

(516) 562-1304 (FAX)

E-mail: smoorji@nshs.edu

Pasquale Razzano MA

Research Assistant, Orthopedic Research Laboratory

North Shore- Long Island Jewish Research Institute

350 Community Drive, Manhasset NY 11030

(516) 562-1150 (Office)

(516) 562-1304 (FAX)

E-mail: prazzano@nshs.edu

Daniel A. Grande PhD

Director, Division of Orthopedic Research

North Shore- Long Island Jewish Research Institute,

350 Community Drive, Manhasset NY 11030 USA

(516) 562-1138

E-mail: dgrande@nshs.edu

James M. Mason PhD

Director, Gene Therapy Vector Laboratory

North Shore-LIJ Research Institute 350 Community Drive

Manhasset NY 11030 USA

(516) 562-1141 (Office)

(516) 562-1304 (FAX)

E-mail: jmason@nshs.edu

ABSTRACT

Improved methods of bone regeneration are needed in the craniofacial rehabilitation of patients with significant bone deficits secondary to tumor resection, for congenital deformities, and prior to prosthetic dental reconstruction. In this study, a gene enhanced tissue engineering approach was used to assess bone regenerative capacity of Sonic hedgehog (Shh) transduced gingival fibroblasts, mesenchymal stem cells, and fat derived cells delivered to rabbit cranial bone defects in an alginate/collagen matrix.

RT-PCR analysis demonstrated that the transduced primary rabbit cell populations expressed Shh RNA. Shh protein secretion was confirmed by ELISA. After six weeks, new full-thickness bone was seen emanating directly from the alginate/collagen matrix in Shh transduced groups. Quantitative two-dimensional digital analysis of histological sections confirmed statistically significant ($p<0.05$) amounts of bone regeneration in all three Shh enhanced groups compared to controls. Necropsy failed to demonstrate any evidence of treatment-related side effects.

This is the first study to demonstrate that Shh delivery to bone defects, in this case through a novel gene enhanced tissue-engineering approach, results in

significant bone regeneration. This encourages further development of the Shh gene enhanced tissue engineering approach for bone regeneration.

INTRODUCTION

Indications for bone grafting in dental and craniofacial reconstruction include bone augmentation prior to prosthetic reconstruction, fracture repair, and repair of facial bone defects secondary to trauma, tumor resection, and congenital deformities. The ideal graft material provides a source of cells capable of forming bone when suitably induced, provides the appropriate signals to induce bone formation (an osteoinductive environment), and provides a scaffold for new bone formation (an osteoconductive environment).

Gene-based therapies involve delivering a specific gene to target tissue with the goal of changing the phenotype or protein expression profile of the recipient cell. Our goal was to employ a gene-enhanced tissue engineering approach to develop a bone grafting material that would prove effective at regenerating both small and large osseous defects of the craniofacial region. The ultimate goal of gene-enhanced tissue engineering is to recapitulate the stages of bone regeneration to produce bone that is indistinguishable from normal host bone.

The regulation of bone metabolism is mediated by both systemic and local factors[1]. Of these, the bone morphogenetic proteins and Sonic hedgehog appear

to be key regulators involved in the formation of new bone, both embryologically and in the repair of fractures.

BMPs are a family of morphogens that regulate bone formation and promote fracture healing, in part by stimulating the differentiation of non-committed precursor cells into osteoblasts[2]. While studies involving the use of exogenously administered recombinant BMP-2 and BMP-7 to induce bone regeneration have generally been promising in lower animals[3,4,5], human studies have demonstrated a large variation in response to recombinant BMP[6]. Additionally, the short in vivo half-life of rBMPs[7], coupled with the ability of pharmacologic doses of BMPs to stimulate osteoclast production[8], may limit the usefulness of recombinant BMPs in the clinical setting[9].

Sonic hedgehog (Shh), a 45 kD vertebrate homologue of the Drosophila segment polarity gene (Hedgehog) and a member of the Hedgehog gene family (Sonic, Desert, and Indian Hedgehog), is a key protein involved in craniofacial morphogenesis. Shh causes differentiation of pluripotent mesenchymal stem cells into osteoblastic lineage by upregulating BMPs via Smad signaling[10]. Shh also induces cell proliferation in a tissue-specific manner during embryogenesis via the regulation of epithelial-mesenchymal interactions (e.g. hair follicles[11] and teeth[12,13]).

The importance of Shh to craniofacial morphogenesis has been demonstrated in experiments with Shh null mutant mice in which the first branchial arch, which

gives rise to both the mandible and maxilla, fails to form[14]. Moreover, mutations in the human Shh gene have been shown to cause holoprocencephaly[15], a developmental field defect in which the cerebral hemispheres fail to separate into distinct halves. Associated anomalies include hypotelorism, midline cleft lip/palate, proboscis-like nasal structures, and premaxillary agenesis. Mutations of the Shh gene have been identified in the rare dental anomaly, solitary median maxillary central incisor[16]. Excess Shh leads to a mediolateral widening of the frontonasal process and hypertelorism[15].

Shh increases the commitment of pluripotential mesenchymal cells into the osteoblastic lineage[10,17] by stimulating the expression of a cascade of downstream genes involved in bone development[18,19,20]. Transduction of an Shh-coding adenovirus into mouse embryo induces the ectopic expression of BMP4, Patched-1, Patched-2, and Gli1[21]. Ectopic bone formation can be induced in athymic mice by transplantation of Shh-transfected chicken fibroblast cells*17*. Implantation of Shh-enhanced chicken embryo-derived dermal fibroblasts into nude mice results in ectopic cartilage and bone formation[22]. However, intramuscular transplantation of Shh protein alone does not induce bone formation[23]. This suggests that either the in vivo half-life of Shh is too short to establish the gradient required of Shh to exert it's effect*24*, or that Shh must function in concert with other downstream factors involved in bone regeneration.

Shh induces the expression of multiple BMPs thus mimicking the complex mixture of BMP heterodimers normally present in developing bone. We expected that the Shh transduced cells would secrete Shh, resulting in the co-ordinated downstream expression of multiple bone growth factors implicated in bone repair and regeneration, including the BMPs. Genetic enhancement of cells with Shh should result in better bone repair than methods employing direct protein delivery or genetic enhancement approaches using individual BMPs.

In this study, the Shh gene from human fetal lung tissue was cloned into the replication incompetent retroviral vector expression series LN[25]. The rat beta-actin enhancer/promoter was engineered to drive expression of Shh. In order to identify a cell population having the best osteogenic potential, three different primary cell populations: gingival fibroblasts, fat-derived stem cells and periosteal-derived cells were genetically enhanced with the Shh vector. Shh expression was confirmed in transduced cells at the RNA and protein levels by RT-PCR and ELISA. Cells were introduced into adult (age 6 months, weighing 2.8 to 3.4kg) male New Zealand White rabbit calvarial defects using a novel alginate/type I collagen composite bone graft matrix. A total of eight groups (N=6) were examined: unrestored empty defects, matrix alone, matrix plus the three cell populations transduced with both control and Shh expression vectors. The bone regenerative capacity of Shh gene enhanced cells was assessed grossly, radiographically and histologically at 6 and 12 weeks post-implantation

RESULTS

Cloning of Human Shh cDNA

Shh is highly expressed in fetal lung tissue. This tissue was used as the source of total RNA for cDNA cloning of Shh by RT-PCR.[26] Due to the high GC content of the Shh cDNA, it was not possible to isolate an undeleted Shh cDNA as a single contiguous fragment. Instead, the Shh cDNA was assembled using conventional molecular biology techniques from five smaller fragments. In one particularly unstable GC rich section of the Shh gene, silent mutations were incorporated into the nucleotide sequence to reduce the GC content without altering the amino acid sequence (see Table 1). With this exception, DNA sequencing of the entire Shh 5' untranslated region and coding sequence confirmed the reported human Shh sequence.[27]

Retroviral Vector Plasmid and Particle Generation

Amphotropic retroviral vector particles harboring LNCX (Neo control vector) and LNB-Shh were generated from cloned producer cells lines at high titer. The β actin enhancer/promoter was chosen for driving expression of Shh because it is a weaker "housekeeping" enhancer/promoter than the strong viral cytomegalovirus (CMV) enhancer/promoter, which often causes toxic overexpression of potent cytokines and morphogens[28]. Thus we have performed limited dosing experiments by testing strong and weak enhancer/promoters to drive transgenes in primary mesenchymal stem cells and other cells in vitro. We found that the β-actin enhancer/promoter is preferred due to its reasonable

expression levels with resultant lack of toxicity. The Moloney murine leukemia virus LTR is used to drive expression of the neomycin resistance gene in both vectors (Figure 1).

Reverse-Transcriptase- Polymerase Chain Reaction (RT-PCR) Analysis of Shh Expression

Shh RNA expression was confirmed in the 3 transduced cell lines by RT-PCR using vector-specific primers. The results (Figure 2) showed that the LNB-Shh transduced periosteal cells expressed Shh at the RNA level while control-transduced cells did not. The gingival fibroblasts and fat-derived cells gave similar results. Controls included GAPDH for RNA integrity and reverse transcription positive controls; no template as negative control and plasmid DNA as the PCR positive control.

Shh Protein Production by Enzyme-Linked Immunosorbent Assay (ELISA)

Forty-eight hour low serum conditioned media was used in ELISA. Shh transduced periosteal stem cells secreted the greatest amount of Shh (Figure 3). This is comparable to the level of BMP production previously observed in osteochondral defect studies using LNB-BMP-7 transduced periosteal-derived cells[29]. Background levels were minimal in control-transduced cells.

Assembly Of Alginate/Type I Collagen/Cell Composites and Assessment of in vitro Viability

Several different materials and various combinations of materials were assessed for use as a matrix prior to selection of the alginate/type I collagen mixture. Matrigel (BD Biosciences, Franklin Lakes, NJ), gelatin, agar, Gelfoam (Johnson and Johnson, Summerville, NJ), and BioOss (Luitpold Pharmaceuticals, Shirley, NY) all gave inferior handling and cell compatibility properties compared to the alginate/type I collagen composite material.

Alginate is a biodegradable polysaccharide composed of mannuronic and guluronic acid units. The porous nature of alginate gels allows for the migration of cells and regulatory proteins inside the network[30]. The alginate used in these studies was from *Macrocystitis pyrifera* (kelp) with a medium viscosity and is composed of 61 % mannuronic and 39 % guluronic acid and a molecular weight of ~100,000 Daltons.

Type I collagen (1%) was added to increase the osteoconductive potential of the alginate[31].To assess the viability of cells in this alginate/type I collagen composite bone graft material, composites were prepared and submitted for histological sectioning immediately after assembly (time 0) and after 7 days in culture. Cells were evenly distributed throughout the graft material at time 0 (Figure 4A). Although cells were not cultured in the graft material prior to implant into defects, it was necessary to first demonstrate that the graft material was biocompatible. After one week in culture, the cells were healthy and had expanded in clusters

throughout the graft (Figure 4B), demonstrating the suitability of this graft material.

Bone Regeneration at 6 and 12 Weeks

Figure 5 is representative of results at 6 weeks for all cell types. Empty defects, matrix alone, and control transduced cells show minimal levels of bone regeneration. Conversely, Shh transduced cells show very substantial levels of bone regeneration radiographically.

For a more quantitative assessment of bone regeneration, composite photomicrographs were assembled from histological sections that were taken through the center of the defects. Only a thin layer of fibrous connective tissue formed in the unrestored empty defect group (Figure 6A). Matrix alone (without cells) integrated into the defects, but again there was only minimal bone formation (data not shown). However, in all matrix-containing groups, the thickness of the defect space was effectively preserved. The defects restored with control-transduced cells plus matrix demonstrated only minimal bone formation (Figure 6B). At higher magnification, control transduced cells within the matrix could still be seen after 6 weeks in vivo.

Conversely, Shh gene-enhancement of the periosteal-derived cells resulted in the formation of fine trabeculae of new bone, primarily along the edges of the defect (Figure 6C). This new bone was composed of fine trabeculae, and had a somewhat delicate appearance. The Shh-enhanced fat-derived stem cells appeared to form relatively thick trabeculae of bone, but this new bone was not

well dispersed throughout the defect (Figure 6D). Even dispersal of new bone was complicated by the observation that the use of fat-derived stem cells often resulted in growth of cyst-like structures in both the control transduced and gene-enhanced groups. These cyst-like structures were not seen with periosteal derived cells or gingival fibroblasts.

The best results were seen with the Shh-transduced gingival fibroblasts, where a substantial amount of new bone formation formed throughout the matrix (Figure 6E). Equally significant was the thickness of this new bone. On high power histologic examination, the new bone was shown to be emanating directly from the matrix (Figure 7).

Results at 12 weeks (Figure 8A-E, Figure 9A-D) were similar to the findings at 6 weeks. Consistent with the 6 week data, the best 12 week results were seen with the Shh-enhanced gingival fibroblasts, where near full thickness bone formation was seen throughout the defect. At higher magnification, significant new bone formation and bone marrow was evident (Figure 10).

Quantitative digital analysis of histological sections was performed and the total 2-dimensional amount of new bone was determined using Adobe Photoshop. A comparison of bone regeneration at 6 weeks versus 12 weeks showed statistically significant new bone formation in all three Shh-enhanced cell lines at both time points compared to controls (Figure 11).

Finally, regarding the safety of stably transducing cells to express Shh in vivo, autopsies performed on Shh-transduced rabbits failed to demonstrate any evidence of treatment-related side effects after 12 weeks.

DISCUSSION

The adult rabbit calvarial "critical size defect" model was chosen because the cranial bones, like the maxilla and mandible, are formed through intramembranous ossification[32,33]. This model has been extensively investigated and characterized with regards to its intrinsic bone healing capacity[34].

Based on the early work of Frame[34], a critical size calvarial defect (CSD; defined as a defect that will not heal completely during the life span of the animal) in the adult rabbit was determined to be 15 mm in diameter, when examined 24 weeks post surgery.

However, the concept of CSD is in flux. Because most studies are of limited duration and do not extend over the life of the animal, the CSD is now being re-defined as the size of the defect that does not heal over the length of the study[35]. Previous definitions of CSD were based on a two-dimensional, linear measurement of bone formation, and did not take into account the overall thickness of the new bone. Consequently, cranial defects that developed a continuous, even if very thin, shelf of bone over the surgical site were considered healed. However, the most important parameter of success in bone healing is the

total three-dimensional amount of new bone deposited in the defect, because the goal in most craniofacial applications of bone regeneration is to restore the site to its original three-dimensional state. Therefore, an 8mm defect size was chosen since there is ample evidence[36] to suggest that this sized defect does not heal spontaneously over a 12-week period.

Our results clearly demonstrate that minimal bone regeneration occurred in empty 8mm defects which validates this size defect for study of bone regeneration at time points up to 12 weeks. Regarding control groups, we chose to use control transduced cells as the best control group for these studies. Control transduced cells were genetically enhanced with the neomycin resistance gene and selected in G418. Shh transduced cells were treated identically as control cells with the exception that the vector they were transduced with contained the Shh gene driven from the beta actin promoter in addition to the neomycin resistance gene. We chose not to use non-transduced cells as a control because in previous experiments in which non-transduced cells were used, there was no statistical difference in bone regeneration between the control transduced and non-transduced groups[37]. Consequently, the control transduced cells serve as the most suitable control for these studies.

The matrix is a critical component of any tissue engineering protocol involving anchorage-dependent cells. Ideally, the matrix should be easy to handle, allow for adherence of cells, and provide a three-dimensional scaffold of sufficient strength to hold the defect space. It must also be porous enough to allow for the

free diffusion of cells and growth factors. Purified bovine collagen is biocompatible, and because it promotes the mineralization process, it is also osteoconductive. However, we found that a collagen-based system alone did not afford a matrix with the requisite strength to hold the defect space. Moreover, collagen gels tend to contract and lose their shape and consistency after as little as 12 hours in culture[38].

Alginate hydrogels are used extensively in cell encapsulation and tissue engineering applications[39] because of their structural properties and good biocompatibility[40]. The porous nature of alginate gels allows for the migration of cells and cytokines inside the network. Bone marrow stromal cells embedded in alginate alone have been used to regenerate rabbit osteochondral defects [38]and sheep cranial defects[41], with no evidence of a host immune response. While alginate gels alone support cell proliferation, proliferation can be enhanced by the addition of an osteoconductive material to the matrix[42].

Our results demonstrate improved bone regeneration through use of a novel alginate/type I bovine collagen-based matrix in which the alginate provides a structural mesh around the cells and the collagen supplies the desired osteoconductive properties to the graft.

Variations in the signaling range of Shh appear to be due to tissue-specific differences in intracellular processing and tissue-restricted expression of binding proteins. This suggests that the ability of cells to respond to Shh may be dependent on the stage of differentiation of the particular cell, with only immature

pluripotential cells being capable of differentiating into an osteoblastic lineage[10]. Consequently, three cell types originating from different tissues were analyzed: gingival fibroblasts, fat-derived stem cells and periosteal-derived cells. All of these cell types are in plentiful supply and easily harvested. Gingival fibroblasts can be induced to express an osteoblastic phenotype[43,44]. Tissue obtained by liposuction contains a mesenchymal stem cell-like population (fat-derived stem cells) that can be induced to differentiate into bone when placed in an appropriate medium[45]. Periosteal-derived cells were selected because of their proven ability to repair bone defects when transfected with BMP-expressing retroviral vectors[28].

The selection of the number of cells implanted per defect ($2x10^6$ cells) was based on the dose-response curves of Gysin et al[46], who demonstrated that the optimum cell count for an 8 mm calvarial defect was $1\text{-}2x10^6$ BMP-expressing cells. However, our results suggest that this total cell count may be insufficient for complete bone regeneration by 12 weeks. In some areas where new bone formation was not complete, the remaining matrix had a lower density of cells. Increasing the concentration of cells should result in faster and more complete bone regeneration.

The use of gene-enhanced tissue engineering overcomes the limitations associated with the one-time delivery of a bolus of protein by providing a sustained, local delivery of protein factors. We demonstrated that Shh delivery to bone defects, in this case through a novel gene enhanced tissue-engineering

approach, resulted in significant bone regeneration. It is important to note that all three cell types, selected for use in these studies because of their reported bone regenerative capacity, were capable of regenerating bone but only when genetically enhanced with Shh. In addition, although the Shh-gene enhanced fat derived stem cells proved useful in bone regeneration, the unexpected cyst formation observed with the use of these cells may prove detrimental to long term bone regeneration. Therefore, we view the Shh-gene enhanced gingival fibroblasts as being the best choice for future use in GETE as substantial amounts of new bone formation was evident throughout the matrix.

In this study, a replication incompetent retroviral expression vector based on the LN series[47] was used. In this vector, the relatively weak rat beta-actin enhancer/promoter was used to drive expression of Shh. Overexpression of potent morphogens under control of the stronger CMV enhancer/promoter or from other transient expression systems that grossly overexpress transgenes can be toxic. The retroviral vectors used in this study are engineered for sustained local delivery of physiologic levels of the expressed gene. Other systems could have been used which result in local presence of supraphysiologic levels of protein for relatively short periods of time, but this would not mimic what occurs during the normal course of development during early skeletogenesis; a process we are trying to emulate. Although the retroviral vector system was used in this study, other gene delivery systems that result in sustained presence of physiological levels of transgene expression can also be used in future studies.

In conclusion, this is the first study to demonstrate that Shh delivery to bone defects, in this case through a novel gene enhanced tissue-engineering approach, results in significant bone regeneration. This encourages further development of the Shh gene enhanced tissue engineering approach for bone regeneration.

MATERIALS AND METHODS

Approval of Experimental Protocols

The protocol was approved by the North Shore- Long Island Jewish Health System Institutional Biosafety Committee. Animal protocols were approved by the North Shore- Long Island Jewish Health System Institutional Animal Care and Use Committee.

Isolation and Culture of Primary Cell Populations

Rabbit Periosteal-Derived Cells: Rabbit periosteum was harvested from the anteromedial surface of the proximal tibia of male New Zealand White rabbits. A rectangular incision was made to expose the bone and periosteum was separated from underlying bone. Only the cambium layer was harvested (confirmed by histological observation). Harvested periosteum was diced into 1 mm cubes and cultured in SDMEM media (composed of high glucose DMEM supplemented with 10 % heat inactivated fetal bovine serum, 1x antibiotic/antimycotic, 12 mM HEPES, 0.4 mM L-proline, and 50 mg/L ascorbic acid).

Fat-Derived Stem Cells: Fat tissue was harvested from the inguinal and abdominal regions of male New Zealand White rabbits. The tissue was placed in SDMEM and digested with 0.075 % collagenase/DNAse mixture at 37^{o}C in a 5 % CO_2 incubator for 1 hr. The cell suspension was then filtered through a 100 nm NYTEC filter, the cells centrifuged, washed twice, and cultured in SDMEM.

Gingival Fibroblasts: Gingival tissue was harvested from the palate of male New Zealand White rabbits. The tissue was cut into 1 mm explants and cultured in SDMEM at 37^{o}C in humidified 5 % CO_2.

Construction of Retroviral Expression Vectors

The Shh cDNA, isolated from human fetal lung tissue, had previously been cloned into the retroviral expression vector LNCX, based on the LN series of vectors in which the murine leukemia virus retroviral LTR drives expression of the neomycin resistance gene.[47] In the retroviral vector plasmid pLNB-Shh, the Shh cDNA was cloned as a HindIII/ClaI fragment replacing the BMP-7 HindIII/ClaI fragment in plasmid pLNB-BMP-7. The rat β-actin enhancer/promoter, a relatively weak housekeeping promoter with low-level constitutive expression, was chosen to drive expression of Shh because expression of potent morphogens from this promoter is not toxic to cells. The retroviral vector plasmids were $CaPO_4$ transfected into GP+E 86 cells.[48] Retroviral vector particle containing conditioned media was collected 48 hr post-transfection and used to transduce PA317 cells in the presence of 8 μg/ml polybrene.[49] PA317 cells were selected for 10-12 days in D10 medium supplemented with 300μg/ml active neomycin analog G418. Amphotropic retroviral vector particles were collected from a cloned producer cell line having a titer of ~1x10^{6} Neo CFU/ml.

Transduction and Selection of Cells

Cells were transduced at ~25 % confluence in 6 well dishes using 400 ul of retroviral vector particles and 1.6 ml D10 supplemented with 8 ug/ml polybrene. Two separate transductions were performed overnight on consecutive nights. Kill control experiments determined that the 10 day selective conditions for rabbit MSC, FSC, and GF are 600, 1800, and 900 ug/ml active G418, respectively. Populations of resultant G418 selected rabbit cells were used in all studies.

RT-PCR Analysis of Shh Expression

Total RNA was isolated from ~1 x 10^6 transduced cells using the RNeasy kit (Qiagen). First strand synthesis was performed using the Reverse Transcription System (Promega). Shh RT-PCR was performed using Herculase Hot Start Enhanced DNA Polymerase (Stratagene) at an annealing temperature of 68^{o}C. Oligonucleotide PCR primers NS186 5' gctctacagcgacttcctcactttcctggaccg 3' (forward primer in coding sequence of Shh) and NS239 5' ccctttttctggagactaaataaaatc 3' (reverse primer downstream of the Shh gene in the viral vector) were used to amplify a 735 bp fragment encompassing the 3' end of Shh and flanking vector sequence encoded specifically by LNB-Shh. Other controls included plasmid pLNB-Shh template as a positive control and a no template control. GAPDH primers NS159 (5' ggtcatccctgagctgaacg 3') and NS160 (5' ttcgttgtcataccaggaaat 3') at an annealing temperature of 54^{o}C were used as control of RNA quality.

Enzyme-Linked ImmunoSorbent Assay of Shh Secretion By Transduced Cells

Cells were grown to confluence in SDMEM supplemented with G418 at a concentration of 1-4 x10^6 total cells. A 48-72-hour conditioned, low serum media (Optimem; Gibco) was harvested from the three cell lines (gingival fibroblasts, periosteal and fat-derived stem cells) carrying the LNCX or LNB-Shh constructs. Indirect enzyme-linked immunosorbent assays (ELISAs) were performed by adding 100ul of conditioned media into 96-well flat-bottom Maxisorp plates (Nunc, Roskilido, Denmark). All assays were performed in triplicate. Antigen was bound at 37^{o}C for 1 hour, blocked with 200ul PBS-T (Phosphate Buffered Saline with 0.1% Tween-20) for 1 hour at room temperature, and then washed three times with PBS-T. The primary antibody, goat IgGanti-mouse Shh amino-terminal peptide (100ug/ml; R&D Systems; Minneapolis, MN), was diluted 1:100 in PBS-T, and 100ul was added per well for 2 hours at room temperature. Three washes with PBS-T, were followed by development using a biotinylated secondary antibody (mouse anti-goat IgG biotinylated antibody; Vectastain ABC kit, Vector Laboratories; Burlingame, CA) and horseradish peroxidase conjugate (Vectastain ABC kit). The chromogenic substrate tetramethylbenzidine (TMB Microwell Peroxidase Substrate; KPL, Gaithersberg, MD) was used for color development. The plates were read at OD450 using a model 400 ATC ELISA plate reader (SLT Lab Instruments; Grodig, Austria). Unconditioned Optimem was used as background control.

Assembly of Gene-Modified Cell–Alginate-Collagen Matrix Constructs

A solution of purified Type 1 bovine collagen (Vitrogen 100, 3.1mg/ml collagen; Cohesion, Palo Alto, CA) was prepared by adding 800 ul of Vitrogen 100 to 100 ul of 10x PBS, followed by the addition of 100 ul of 0.1m NaOH.

The gene-modified cell lines were trypsinized and the cell pellets were resuspended in a 50ml Falcon tube (Becton Dickinson; Lincoln Park, NJ) in 200ul of 2.0% alginic acid (sodium salt, medium viscosity, from Macrocystis pyrifera; Sigma, St. Louis, MO). The cell-alginate solution was added to 200 ul of the above prepared Type 1 collagen preparation. Initial gelation was accomplished by placing the cell-alginate-collagen amalgam at 37^{o}C for 30 minutes. Gelation of the alginate was completed by adding 4ml of 100mM $CaCl_2$ directly to the amalgam. The matrix was allowed to gel for 15 minutes and then rinsed 3 times with PBS prior to implantation.

Surgical Procedures

A total of 24 adult male (age 6 months) New Zealand White rabbits, weighing 3.0 to 4.0 kg, were used in this study. The rabbits were kept in standard laboratory double cages with a 12-hour day/night cycle and an ambient temperature of 21^{o}C. The rabbits were permitted two hours free housing per day, and had access to tap water and food pellets.

Food and water were withheld from the rabbits for 6 hours and 1 hour respectively prior to surgery. A total of 0.4cc/3 kg of Tazidine was administered 18 hours prior to surgery by means of intramuscular injection, Animals were pre-

anaesthetised with an intramuscular injection of 5mg/kg acepromazine, and induced with 12.5mg/kg ketamine and 4% Isoflurane. Adequateness of anaesthesia was assessed by the absence of withdrawal reflex to toe pinch and the absence of corneal reflex.

In each animal, the surgical field was shaved and prepped with iodophor. Following the infiltration of local anaesthesia (2% lidocaine with 1:100,000 epinephrine), midline sagittal incisions were extended from the occipital region to the bridge of the nose. Subperiosteal dissections were performed anteriorly and posteriorly to expose the frontal and parietal regions of the cranium. Using a trephine bur with copious saline irrigation, four full thickness 8mm bone defects were created. Great care was taken to avoid perforating the underlying dura. The surgically created defects were restored with the selected transduced cells in the alginate matrix or the corresponding controls. The scalp tissues were reapproximated to the remaining calvarium, and sutured with 4-0 Vicryl sutures. Post-operative analgesia was accomplished by administering 0.1 mg/kg Buprenex subcutaneously q12h for the first 48 hours.

After 6 or 12 weeks, the animals were anesthetized with ketamine and sacrificed by means of a pentobarbital overdose.

Experimental Groups

The experimental groups comprised allogenic gingival fibroblasts, periosteal and fat-derived stem cells transduced with the replication incompetent Shh retroviral vector (LNB-Shh) and control vector (LNCX). Additional controls included

alginate/collagen matrix alone and empty defects , for a total of 8 groups. Twelve calvarial defects (6 per time/group) were analyzed for each experimental group.

Radiographic Analysis of Bone Defect Healing

Post mortem radiographs (Kodak Ultraspeed DF-50 Dental Film) were taken of the sectioned calvaria using a portable x-ray unit (Philips Dens-o-Matic, 65 kVp, 7.5 mAmp, 1.5 seconds).

Histological Analysis

The defect sites were identified visually, and then sectioned into halves. One half was decalcified in **"**overnight bone decalcification" solution (Decal Corporation, Tallman NY) for 3 days. After embedding in paraffin, 4um serial sections were obtained, and stained with hematoxylin and eosin.

When processing the alginate/collagen/cell matrices for histologic examination, 10 mM $CaCl_2$ was added to the formalin during the initial fixation period to prevent depolymerization of the alginate matrix. The matrices were then fixed overnight with 50 mm $BaCl_2$ at 4^0C to permanently cross-link the alginate prior to final processing.

Quantitative digital analysis of histological sections was performed. Digitized composite photomicrographs were analyzed on an IBM PC running Windows 98 with Adobe Photoshop 6.0. The mineralized area of the defects in the digitized radiographs was identified by the value of the pixel in the image. The percentage of area of mineralized tissue within the defect size was determined.

Statistical Analysis

Determination of *n* (the minimum sample size to provide proper discriminatory capability) for in vivo animal studies was done by power analysis. A sample size of 6 would yield 80% power to detect a difference of 10% between the two groups (case vs. control) using a 2-tailed, paired t-test with a 0.05 significance level. One-way Analysis of Variance was followed by Bonferroni pairwise multiple comparison. A “p” value of less than 0.05 was considered statistically significant.

Acknowledgements

We are grateful to Enesa Paric for technical assistance with the cell culture. We would also like to thank Yana Moses for preparation of the histological sections.

TABLE 1: Oligonucleotide primers used to generate complete Shh cDNA

NS145 F 5' aaaaagcttgggcgagatgctgctgctggcgagatgtct 3'	404 bp
NS182 R 5' tcgtcccagccctcggtcacccgc 3'	
NS181 F 5' gcgggtgaccgagggctgggacga 3'	359 bp
NS115 R 5' aggaaagtgaggaagtcg 3'	
NS198 F 5' accgcgtgctggcggcggacgaccaggg 3'	520 bp
NS199 R 5' tgtgcgcgcgggcgccagtgcagccaggagcgcg 3'	
NS189 F 5'cccgcgcgcacAgaTAgAggAggAgaTagTggTggAggTgaTAgAggAggTggTggAggAagagtagccctaaccgctccaggtgctgccg 3'	
NS190 R 5' cggcagcacctggagcggttagggctactctTccTccAccAccTccTcTAtcAccTccAccActAtcTccTccTcTAtcTgtgcgcgcggg 3'	
NS200 F 5' ctccaggtgctgccgacgctccgggtgcgg 3'	148 bp
NS146 R 5' tttatcgattcagctggacttgaccgccatgcccagcgg 3'	

Silent mutations (capital letters) were created in the Shh coding sequence of primers NS189 and NS190, which were annealed together to generate a 91 bp fragment. The mutations were needed to reduce the GC content of this region of Shh, which was unstable in the constructs. All other primers were used in RT-PCR to generate the PCR fragment lengths indicated.

Figure 1. Retroviral Expression Vectors Used. LTR: long terminal repeat, Neo^r: neomycin resistance gene; ß-act: rat beta- actin promoter; Shh: Sonic hedgehog gene. Constructs are based on the LN series containing the selectable neomycin resistance gene driven by the 5' LTR. These retroviral vectors are generated as amphotropic retroviral vector particles from PA317 cells. Sizes of genomic length RNA and mRNA are indicated.

Figure 2. Reverse Transcriptase- Polymerase Chain Reaction (RT-PCR) Analysis of Total RNA Isolated from Periosteal-Derived Cells. Lanes: (M) molecular weight markers, (1) LNCX transduced, (2) LNB-Shh transduced, (3) No template, and (4) plasmid pLNB-Shh. **(A)** *RT-PCR analysis of RNA from periosteal-derived cells.* PCR primers that amplify only vector-specific RNA transcripts were used to generate a 735 bp vector specific Shh PCR product. Note that only LNB-Shh (lane 2) and the positive control plasmid LNB-Shh (lane 4) generate the PCR product. **(B)** *GAPDH control.* GAPDH PCR primers were used to generate a 294 bp GAPDH PCR product as control for RNA integrity and reverse transcription reaction.

Figure 3: Shh Protein Production In Transduced Cells.

Shh protein production in the 3 cell types was assessed by Enzyme-Linked ImmunoSorbent Assay (ELISA) as described in the Materials and Methods. Shh production of LNCX control transduced cells (blue) is compared to the Shh-enhanced cells (red).

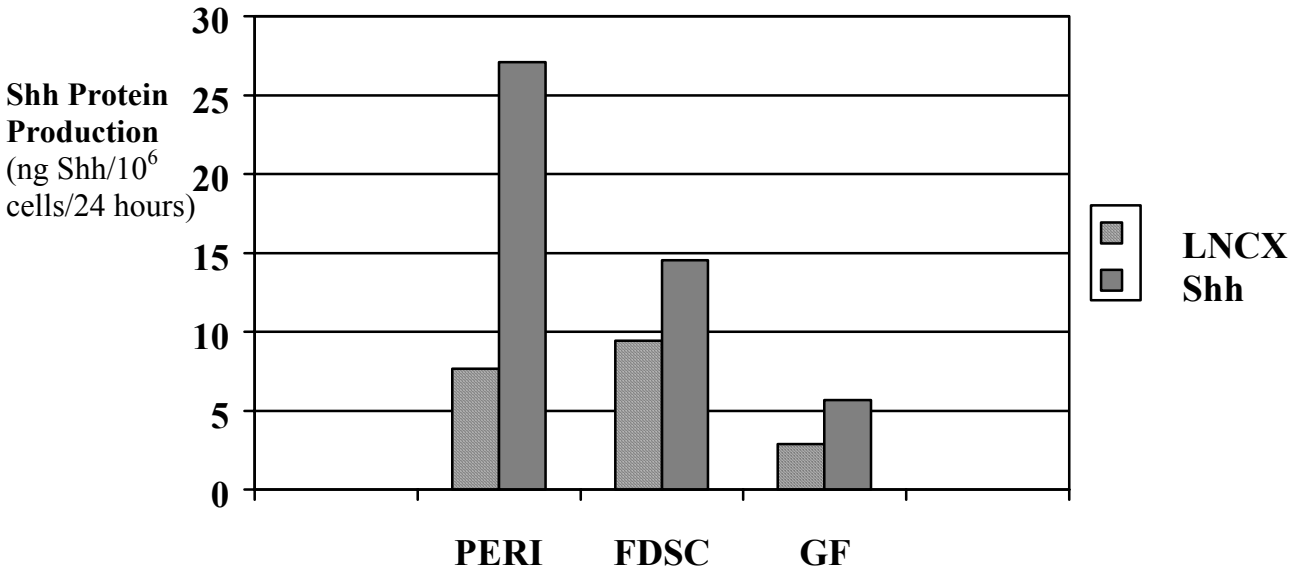

Figure 4. Histology of Alginate/Type I Collagen/ Periosteal-Derived Cell Composite Bone Graft Material. (A) *Alginate/type I collagen / periosteal-derived cell composite graft* with 2 x 10^6 cells/450 ul matrix construct, *Time 0*. **(B)** Similar graft *after 7 days* culture in vitro. Hematoxylin and eosin stain. Original magnification 100x (inset 200x).

Figure 5: Radiographic Analysis Of Calvarial Bone Regeneration At 6 Weeks. Significantly more bone regeneration is evident in the SHH-enhanced gingival fibroblasts (upper right) compared to the 3 controls.

Figure 6: Histologic Assessment of Bone Regeneration at 6 Weeks.

(A) *Unrestored empty defect*. Only a thin band of fibrous connective tissue is present in the defect space. **(B)** *Matrix alone*. The matrix has preserved the thickness of the defect space. New bone formation is minimal. **(C)** *Matrix plus Shh gene-enhanced periosteal-derived cells*. Thin trabeculae of new bone are identified primarily at the surgical margins. **(D)** *Matrix plus Shh gene-enhanced fat-derived stem cells***.** Relatively thick trabeculae of new bone are present, but this new bone is not evenly distributed throughout the defect site. (**E)** *Matrix plus Shh gene-enhanced gingival fibroblasts*. A significant amount of new bone is present throughout the defect space. Hematoxylin and eosin stain. Original magnification 4x.

Figure 7: Histologic Assessment of Bone Regeneration in Shh gene-enhanced gingival fibroblasts at 6 Weeks. Significant new bone formation is evident. The amorphous, purple material represents remaining matrix. Hematoxylin and eosin stain. Original magnification 40x.

Figure 8: Histologic Assessment of Bone Regeneration at 12 Weeks. (A) *Unrestored empty defect*. **(B)** *Matrix alone*. **(C)** *Matrix plus Shh gene-enhanced periosteal-derived cells.* **(D)** *Matrix plus Shh gene-enhanced fat-derived stem cells*. **(E)** *Matrix plus Shh gene-enhanced gingival fibroblasts*. Similar to the findings noted at 6 weeks, the Shh-gene-enhanced cells resulted in the best overall bone regeneration. Hematoxylin and eosin stain. Original magnification 4x.

Figure 9: Histologic Comparison of Bone Regeneration Between Groups at 12 Weeks. (A) *Unrestored empty defect control* shows thin band of fibrous connective tissue. **(B)** In the *matrix-only control*, remaining matrix is identified. **(C)** *Matrix and control transduced gingival fibroblasts*. **(D)** *Shh-gene-enhanced gingival fibroblasts*. Compared to the three controls, significant new bone formation is observed. Hematoxylin and eosin stain. Original magnification 40x.

Figure 10: Histologic Assessment of Bone Regeneration in Shh gene-enhanced gingival fibroblasts at 12 Weeks. Bone formation is seen in direct

continuity with the matrix. Bone marrow is also identified. Hematoxylin and eosin stain. Original magnification 40x.

Figure 11: Bone Rgeneration in Calvarial Defects After 6and 12 Weeks.

Histologic slides were digitized and the total 2-dimensional amount of new bone in defects was quantitated using Adobe Photoshop. Data was analyzed using One-Way Analysis of Variance (ANOVA) followed by Bonferroni pairwise multiple comparison. In all cases, Shh gene enhancement of cells resulted in statistically significant differences ($p<0.05$) compared to controls.

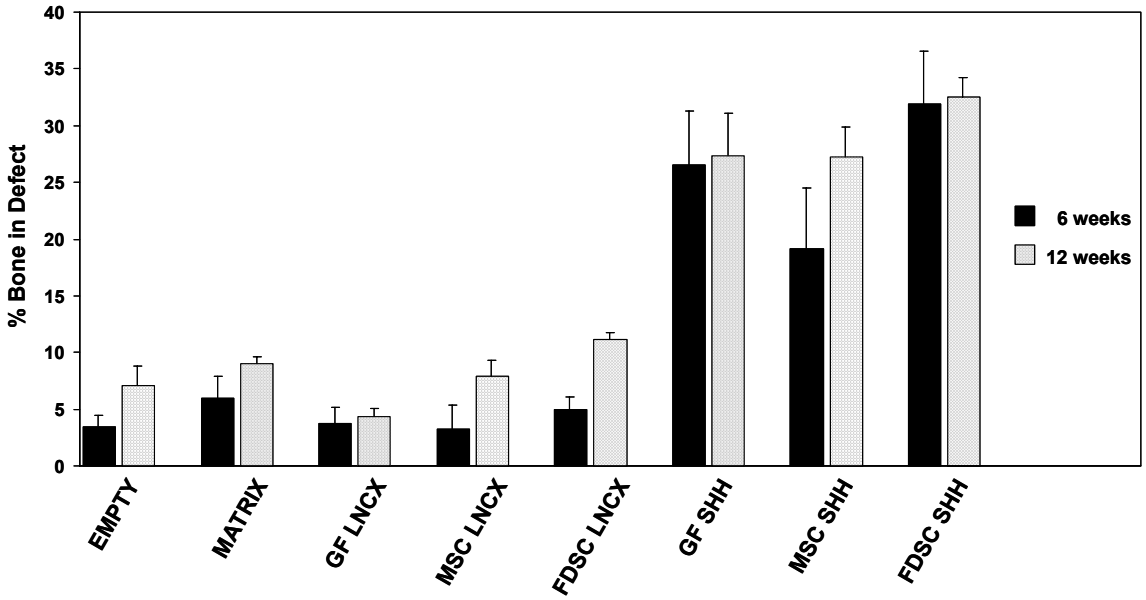

REFERENCES

[1] Zellin G. Growth factors and bone regeneration. Swedish Dental Journal 1998: 129; 7-65.

[2] Ebara S, Nakayama K. Mechanisms for the action of bone morphogenetic proteins and regulation of their activity. Spine 2002: 27; S10-S15.

[3] Yoshida K, Bessho K, Fujimura K, Konishi Y, Kusumoto K, Ogawa Y, et al. Enhancement by recombinant human bone morphogenetic protein-2 of bone formation by means of porous hydroxyapatite in mandibular bone defects. J Dent Res 1999: 78; 1505-1510.

[4] Miyaji H, Sugaya T, Miyamoto T, Kato K, Kato H. Hard tissue formation on dentin surfaces applied with recombinant human bone morphogenetic protein-2 in the connective tissue of the palate. J Periodont Res 2002: 37; 204-209.

[5] Suzuki T, Bessho K, Fujimura K, Okubo Y, Segami N, Iizuka T. Regeneration of defects in the articular cartilage in rabbit temporomandibular joints by bone morphogenetic protein-2. British J Oral Maxillofac Surg 2002: 40; 201-206.

[6] Groeneveld EH, Burger EH. Bone morphogenetic proteins in human bone regeneration. European J Endocrinol 2000: 142; 9-21.

[7] Wozney JM. Overview of bone morphogenetic protein. Spine 2002; 27; S2-S8.

[8] Itoh K, Udagawa N, Katagiri T, Iemura S, Ueno N, Yasuda H, et al. Bone morphogenetic protein 2 stimulates osteoclast differentiation and survival

supported by receptor activation of nuclear factor –κβ ligand. Endocrinology 2001: 142; 3656-3662.

[9] Valentin-Opran A, Wozney J, Csimma C, Lilly L, Riedel GE. Clinical evaluation of recombinant bone morphogenetic protein-2. Clin Orthopaed Rel Res 2002: 395; 110-120.

[10] Spinella-Jaegle S et al. Sonic Hedgehog increases the commitment of pluripotent mesenchymal cells into the osteoblastic lineage and abolishes adipocytic differentiation. J Cell Science 2001: 114; 2085-2094.

[11] St-Jacques B, Dassule HR, Karavanova I, Botchkarev VA, Li J, et al. Sonic hedgehog signaling is essential for hair development. Current Biology 1998; 8: 1058-1068.

[12] Peters H, Balling R. Teeth: where and how to make them. Trends in Genetics 1999: 15; 59-65.

[13] Dassule HR, Lewis P, Bei M, Maas R, McMahon AP. Sonic hedgehog regulates growth and morphogenesis of the tooth. Development 2000: 127; 4775-4785.

[14] Chiang C, Litingtung Y, Lee E, Young KE, Corden JL, et al. Cyclopia and defective axial patterning in mice lacking sonic hedgehog gene function. Nature 1996; 383; 407-413.

[15] Hu D, Helms JA. The role of Sonic hedgehog in normal and abnormal craniofacial morphogenesis. Development 1999: 126; 4873-4884.

[16] Nanni L, Ming JE, Du Y, Hall RK, Aldred M, et al. SHH mutation is associated with solitary median maxillary central incisor: a study of 13 patients and review of the literature. Am J Med Genetics 2001: 102; 1-10.

[17] Kinto N et al. Fibroblasts expressing sonic hedgehog induce osteoblast differentiation and ectopic bone formation. FEBS Letters 1997: 404; 319-323.

[18] Kato M et al. Identification of Sonic Hedgehog-responsive genes using cDNA microarray. Biochem Biophys Res Comm. 2001: 298; 472-478.

[19] Nybakken K, Perrimon N. Hedgehog signal transduction: recent findings. Current Opinion Genet and Develop 2002: 12; 503-511.

[20] Bitgood MJ, McMahon AP. Hedgehog and BMP genes are co-expressed at many diverse sites of cell-cell interaction in the mouse embryo. Dev Biol 1995:172; 126-138

[21] Ohsaki k, Osumi N, Nakamura S. Altered whisker patterns induced by ectopic expression of SHH are topographically represented by barrels. Develop Brain Res 2002: 137; 159-170.

[22] Enamoto-Iwamoto M, Nakamura T, Aikawa T, Higuchi Y, Yuasa T, et al. Hedgehog proteins stimulate chondrogenic cell differentiation and cartilage formation. J Bone Min Res 2000; 15: 1659-1668.

[23] Yuasa T, Kataoka H, Kinto N, Iwamoto M, Enomoto-Iwamoto M, Iemura SI, et al. Sonic Hedgehog is involved in osteioblast differentiation by cooperating with BMP-2. J Cell Physiol 2002: 193; 225-232.

[24] Goetz JA, Suber LM, Zeng X, Robbins DJ. Sonic hedgehog as a mediator of long-range signaling. Bioessays (2002); 24: 157-165.

[25] Miller AD and Rosman GJ. Improved retroviral vectors for gene transfer and expression. Biotechniques 198: 97; 980-990.

[26] Pepicelli CV, Lewis PM, McMahon AP. Sonic hedgehog regulates branching morphogenesis in the mammalian lung. Curr Biol 1998: 8(19); 1083-1086.

[27] Marigo V, Roberts DJ, Lee SMK, Tsukurov O, Levi T, Gastier JM, Epstein DJ, Gilbert DJ, Martin CG, Copeland NG, Seidman CE, Jenkins NA, Seidman JG, McMahon AP, Tabin C. Cloning, expression and chromosomal location of SHH and IHH, two human homologues of the Drosophila segment polarity gene Hedgehog. Genomics 1995: 28; 44-51.

[28] Mason JM, Grande DA, Barcia M, et al. Expression of human bone morphogenetic protein-7 in primary rabbit periosteal cells: potential utility in gene therapy for bone repair. Gene Therapy 1998; 5: 1098-1104.

[29] Grande DA, Tomin A, Mason JM, Wollowick AL, Garrone B, Lane J. A dual gene therapy approach to osteochondral defect repair using a bilayer implant containing BMP-7 and IGF-1 transduced periosteal cells. Trans Orthop Res Soc 2001: 26; 294.

[30] Stabler C, Wilks K, Sambanis A, Constantinidis I. The effects of alginate composition on encapsulated BTC3 cells. Biomaterials 2001: 22; 1301-1310.

[31] Fleming JE, Cornell CN, Muschler GF. Bone cells and matrices in orthopedic tissue engineering. Orthop Clin North Am 2000; 31; 357-374.

[32] Rudert M. Histological evaluation of osteochondral defects; consideration of animal models with emphasis on the rabbit, experimental setup, follow-up and applied methods. Cells Tissue Organs 2002; 171; 229-240.

[33] Hollinger JO, Kleinschmidt JC. The critical size defect as an experimental model to test bone repair materials. J Craniofacial Surg 1990: 1; 60-68.

[34] Frame JW. A convenient animal model for testing bone substitute materials. J Oral Surg 1980: 38; 176-180.

[35] Gosain AK, Song L, Yu P, Mehrara BJ, Maeda CY, Gold LI, et al. Osteogenesis in cranial defects: reassessment of the concept of critical size and the expression of TGF- [beta] isoforms. Plastic Reconsrtuctive Surg 2000: 106-360-371.

[36] Kramer IR, Killey HC, Wright HC. A histological and radiological comparison of the healing of defects in the rabbit calvarium with and without implanted heterogenous anorganic bone. Arch Oral Biol 1968: 13; 1095-1106.

[37] Breitbart AS, Grande DA, Mason JM, Barcia M, James T, and Grant RT. Gene –enhanced tissue engineering: applications for bone healing using cultured periosteal cells transduced retrovirally with the BMP-7 gene. Ann Plast Surg 1999; 42; 488-495.

[38] Diduch DR, Jordan LC, Mierisch CM, Balian G. Marrow stromal cells embedded in alginate for repair of osteochondral defects. J Arthroscopic and Related Surg 2000: 16; 571-577.

[39] Milla E, Barra G, Ramires PA, Leo G, Aversa P, Romoito A. Poly(L-lactide) acid/alginate composite membranes for guided tissue regeneration. J Biomed Mater Res 2001:57; 248-257.

[40] Loebsack A, Greene K, Wyatt S, Culberson C, Austin C, Beiler R. In vivo characterization of a porous hydrogel material for use as a tissue bulking agent. J Biomed Mater Res 2001; 57; 575-581.

[41] Shang Q, Wang Z, Liu W, Shi Y, Cui L, Cao Y. Tissue-engineered bone repair of sheep cranial defects with autologous bone marrow stromal cells. J Craniofac Surg 2001: 12; 586-593.

[42] Miralles G, Baudoin R, Dumas D, Baptiste D, Hubert P, Stoltz JF, et al. Sodium alginate sponges with or without sodium hyaloronate: In vitro engineering of cartilage. J Biomed Mater Res 2001: 57; 268-278.

[43] Murphy MG, Mailhot J, Borke J, Wataha J, Sharawy M, et al. The effects of rhBMP-2 on human osteosarcoma cells and gingival fibroblasts in vitro. J Oral Implantology 2001: 27; 16-24.

[44] Krebsbach PH, Gu K, Franceschi RT, Rutherford RB. Gene therapy-directed osteogenesis: BMP-7 transduced human fibroblasts form bone in vivo. Human gene therapy 2000: 11; 1201-1210.

[45] Zuk PA, Zhu m, Mizuno H, Huang J, Futrell JW, Katz AJ, et al. Multilineage cells from human adipose tissue: implications for cell-based therapies. Tissue Eng 2001: 7; 211-228.

[46] Gysin R, Wergedal JE, Sheng MH, Kasukawa Y, Miyakoshi N et al. Ex vivo gene therapy with stromal cells transduced with a retroviral vector containing

the BMP4 gene completely heals critical size calvarial defect in rats. Gene Therapy (2002): 9; 991-999.

[47] Miller AD and Rosman GJ. Improved retroviral vectors for gene transfer and expression. Biotechniques 198: 97; 980-990.

[48] Markowitz D, Goff S, Bank A. A safe packaging line for gene transfer: separating viral genes on two different plasmids. J Virol 1988: 62; 1120-1124.

[49] Miller AD, Buttimore C. Redesign of retrovirus packaging cell lines to avoid recombination leading to helper virus production. Mol Cell Biol 1986: 6; 2895-2902.

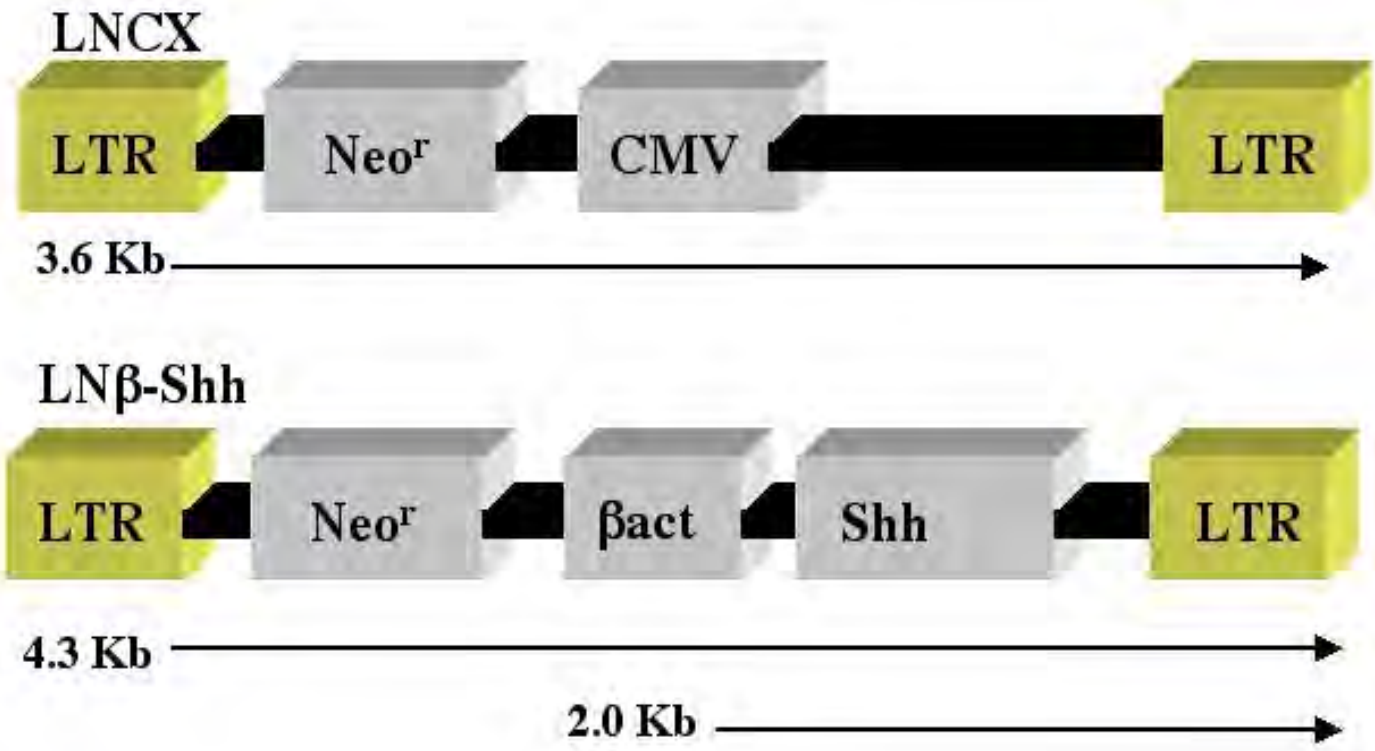
LNCX
LTR
Neo^r
CMV
LTR
3.6 Kb
LNβ-Shh
LTR
Neo^r
βact
Shh
LTR
4.3 Kb
2.0 Kb

A

M 1 2 3 4

1.5kb →

500bp →

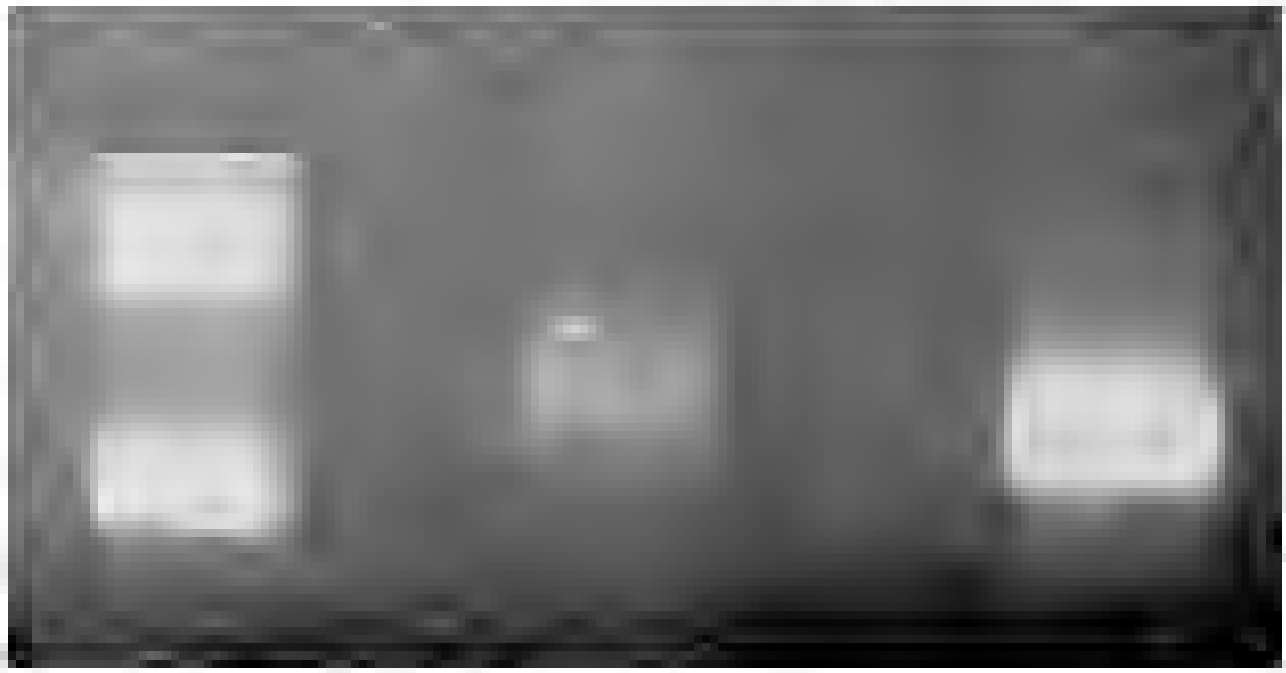

B

500bp →